AJNR

Diffusion-weighted MR imaging of acute stroke: correlation with T2-weighted and magnetic susceptibility-enhanced MR imaging in cats.

M E Moseley, J Kucharczyk, J Mintorovitch, Y Cohen, J Kurhanewicz, N Derugin, H Asgari and D Norman

AJNR Am J Neuroradiol 1990, 11 (3) 423-429
http://www.ajnr.org/content/11/3/423

Diffusion-Weighted MR Imaging of Acute Stroke: Correlation with T2-Weighted and Magnetic Susceptibility-Enhanced MR Imaging in Cats

M. E. Moseley[1]
J. Kucharczyk[1]
J. Mintorovitch[2]
Y. Cohen[2]
J. Kurhanewicz[1]
N. Derugin[1]
H. Asgari[1]
D. Norman[1]

We evaluated the temporal and anatomic relationships between changes in diffusion-weighted MR image signal intensity, induced by unilateral occlusion of the middle cerebral artery in cats, and tissue perfusion deficits observed in the same animals on T2-weighted MR images after administration of a nonionic intravascular T2* shortening agent. Diffusion-weighted images obtained with strong diffusion-sensitizing gradient strengths (5.6 gauss/cm, corresponding to gradient attenuation factor, b, values of 1413 sec/mm^2) displayed increased signal intensity in the ischemic middle cerebral artery territory less than 1 hr after occlusion, whereas T2-weighted images without contrast usually failed to detect injury for 2–3 hr after stroke. After contrast administration (0.5–1.0 mmol/kg Dy-DTPA-BMA, IV), however, T2-weighted images revealed perfusion deficits (relative hyperintensity) within 1 hr after middle cerebral artery occlusion that corresponded closely to the anatomic regions of ischemic injury shown on diffusion-weighted MR images. Close correlations were also found between early increases in diffusion-weighted MR image signal intensity and disrupted phosphorus-31 and proton metabolite levels evaluated with surface coil MR spectroscopy, as well as with post-mortem histopathology.

These data indicate that diffusion-weighted MR images more accurately reflect early-onset pathophysiologic changes induced by acute cerebral ischemia than do T2-weighted spin-echo images.

***AJNR* 11:423–429, May/June 1990**

In vivo diffusion-weighted MR imaging, which measures the microscopic motion of water protons, has been used recently to characterize brain tissue abnormalities caused by cerebral ischemia [1, 2]. Acute stroke, however caused, produces a rapid and progressive disruption of mitochondrial oxidative phosphorylation, with ensuing losses of high energy phosphates and increases in inorganic phosphate and lactate. These metabolic disturbances precipitate glial and neuronal transmembrane Na^+/K^+ transport failure, resulting in a shift of fluid and Na^+ from the extracellular to the intracellular compartment after a latency of only a few minutes [3].

Moseley et al. [2] evaluated the potential of diffusion-weighted MR imaging for early detection of regional cerebral-ischemia-induced edema using a cat model. Diffusion-weighted images were acquired by using very strong gradient strength factors (b values of up to 1413 sec/mm^2). Evidence of cerebral injury could be found as early as 45 min after unilateral occlusion of the middle cerebral artery (MCA) using diffusion-weighted MR imaging, whereas T2-weighted spin-echo images failed to demonstrate clear increases in signal intensity in the MCA territory even 2–3 hr after occlusion. Close correlations were also established between diffusion-weighted tissue signal intensity ratios and metabolic abnormalities measured with surface coil phosphorus-31 and proton MR spectroscopy. These data [2] provided the first evidence that diffusion-weighted MR images accurately reflect early-onset pathophysiologic changes induced by acute cerebral ischemia.

Received October 30, 1989; revision requested December 13, 1989; revision received January 8, 1990; accepted January 8, 1990.

[1] Department of Radiology, Box 0628, University of California, San Francisco, CA 94143. Address reprint requests to M. E. Moseley.

[2] Department of Pharmaceutical Chemistry, University of California, San Francisco, CA 94143.

0195-6108/90/1103-0423

The objective of the present study was to compare the anatomic extent and severity of ischemic brain injury shown on diffusion-weighted MR imaging with tissue perfusion deficits demonstrated by the combined use of a nonionic intravascular T2* magnetic susceptibility contrast agent and conventional T2-weighted spin-echo MR imaging. Diffusion-weighted MR images were also evaluated in relation to assessments of cerebral metabolic injury obtained via surface coil phosphorus-31 and proton MR spectroscopy from the ischemic MCA territory. Finally, histochemical mapping of the viability of the electron transport chain enzymes was carried out with 2-, 3-, and 5-triphenyl tetrazolium chloride (TTC) [4] to correlate spatially the evolution of ischemic tissue injury with the MR imaging/spectroscopy results.

Materials and Methods

Thirteen young adult cats weighing 2.0 to 4.5 kg were anesthetized intravenously with 30 mg/kg Nembutal. Polyethylene catheters were placed in the temporal vein and artery for blood pressure monitoring and drug administration. The right MCA was isolated via the transorbital approach and occluded just proximal to the origin of the lateral striate arteries with bipolar electrocautery followed by complete surgical transection. The dural incision and orbit were covered with a saline-moistened gauze and an absorbable gelatin sponge. The muscles overlying the ipsilateral parietal fossa were excised unilaterally to optimize the placement of the MR-spectroscopy surface coil in a standard location over the MCA territory.

A 2-T chemical shift imager/spectrometer unit (General Electric Medical Systems, Fremont, CA), equipped with GE Acustar self-shielded gradient coils (± 20 gauss/cm, 15-cm bore size) was used. Phosphorus-31 and proton MR spectroscopy was performed with a 2 × 3 cm double-tuned surface coil positioned over the MCA territory after scalp and muscle retraction. MR imaging was performed with an 8.5-cm inner-diameter low-pass birdcage proton imaging coil. The imaging birdcage and surface coils were equipped with a detuning capacitor switch to perform sequential spectroscopy and imaging without changing the position of the animal in the magnet. Successive multislice diffusion-weighted images, MR spectra, and T2-weighted images were obtained for at least 5 hr after occlusion. T2-weighted images, 2800/80, 160 (TR/TEs), with 3-mm slices and 1-mm gap were obtained with a field of view (FOV) of 80 mm in which two scans were averaged for each one of the 128 phase-encoding steps, resulting in a total acquisition time of 12 min. Cardiac-gated and nongated single and multislice coronal and axial diffusion-weighted spin-echo images, 1000–1800/80 (TR range/TE), with 3-mm slices, 1-mm gap, and FOV = 80 mm were acquired with a diffusion-gradient pulse duration of 20 msec along the slice-selection direction, a gradient separation of 40 msec, and very large diffusion-sensitizing gradient (b) values of 1413 sec/mm^2 (gradient strength of 5.6 gauss/cm). These gradients were ramped to avoid excessive dB/dt effects. Four to eight scans were averaged for each of 128 phase-encoding steps, resulting in a total collection time of about 16 min.

Region-of-interest (ROI) image analyses were carried out in the injured middle temporal cortex, ectosylvian gyrus, and caudate nucleus, and compared with the corresponding uninjured contralateral gray matter regions. A signal intensity ratio was calculated as the ROI image intensity ratio of an abnormal, ischemic region over that of the normal, contralateral side.

Phosphorus-31 MR spectra at 34.6 MHz were acquired by single-pulse experiments from 256 signal averages with an effective TR of 2250 and a total acquisition time of 9.6 min. Proton (85.6 MHz) spin-echo spectra (tau = 128 and 192 msec) were acquired with water presaturation, TR of 1750, and 128 signal averages, resulting in a total collection time of 5 min.

MR spectra were phased and analyzed with a line-fitting computer simulation program. The beta, alpha, and gamma peaks for ATP and the peaks for phosphocreatine (PCr), phosphodiester (PD), inorganic phosphate (Pi), and injured inorganic phosphate (Pii) and phosphomonoester (PM) were resolved. The Pii:PCr ratio was calculated to quantify the bioenergetic status of the tissues. From the proton spectra, the peak areas of lactate and N-acetylaspartate (NAA) were resolved and the lactate:NAA ratios calculated. The presence of lactate was confirmed from comparison of tau = 128 msec and tau = 192 msec spin-echo experiments in which the lactate peak is inverted at tau = 192 msec. To compare the MR spectroscopy peak area ratios with the MR imaging tissue contrast values, the ROI chosen were the superior and middle frontoparietal gyri, which correspond anatomically to the cerebral tissues beneath the surface coil.

In order to compare the anatomic region of perfusion deficiency with the areas of high signal intensity on diffusion-weighted MR images, cats were also tested with a nonionic T2*-shortening contrast agent, Dy-DTPA-bis (methylamide) (Dy-DTPA-BMA). The Dy-DTPA-BMA complex was prepared by Salutar, Inc. (Sunnyvale, CA) by refluxing stoichiometric amounts of dysprosium oxide and DTPA-BMA. The contrast agent was infused intravenously over approximately 3 min at doses of 0.5 or 1.0 mmol/kg beginning at phase-encoding step 32 and finishing at step 60 of the T2-weighted image acquisition (Fig. 1). Dy-DTPA-BMA injections were given at different times following MCA occlusion in individual cats. After injection, the magnetic susceptibility effect was evaluated for 15–60 min in both ischemic and normal hemispheres by comparing ROI intensity to precontrast T2-weighted and diffusion-weighted ROI intensities.

At the conclusion of the MR protocol, 15 ml/kg of a 2% solution of TTC was infused transcardially. The brain was removed from the cranium after 10–20 min, immersed in a 2% triphenyl tetrazolium chloride (TTC) solution for another 10–20 min, and then stored overnight in 10% buffered formalin in a light-shielded container. Twenty-four to thirty-six hours later the brain was sectioned coronally at 2–3 mm and immediately examined for histologic evidence of ischemic damage. TTC stains normal brain tissues red and injured tissues pink (ischemic) to gray-white (necrotic) [5].

Results

Detection of Ischemic Injury with Diffusion-Weighted MR Imaging

Corresponding diffusion- and T2-weighted spin-echo images, taken within 1 hr after occlusion (Fig. 2, left panels) and

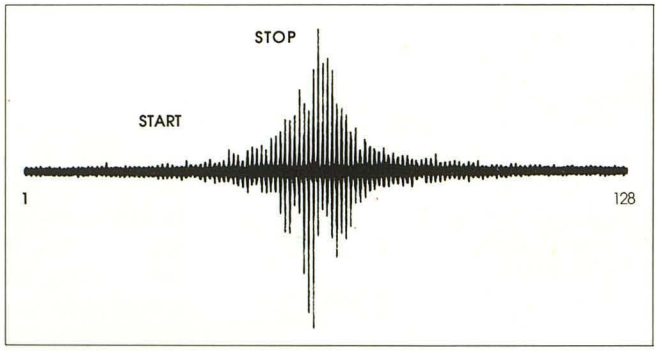

Fig. 1.—Method of collection of contrast-enhanced T2-weighted spin-echo signal (12-min acquisition) images. The time of administration of Dy-DTPA-BMA contrast during the 128 phase-encoding step sequence was between scans 32–60 in order to maximize plasma contrast concentration during the most sensitive stage of signal acquisition (scans 40–80).

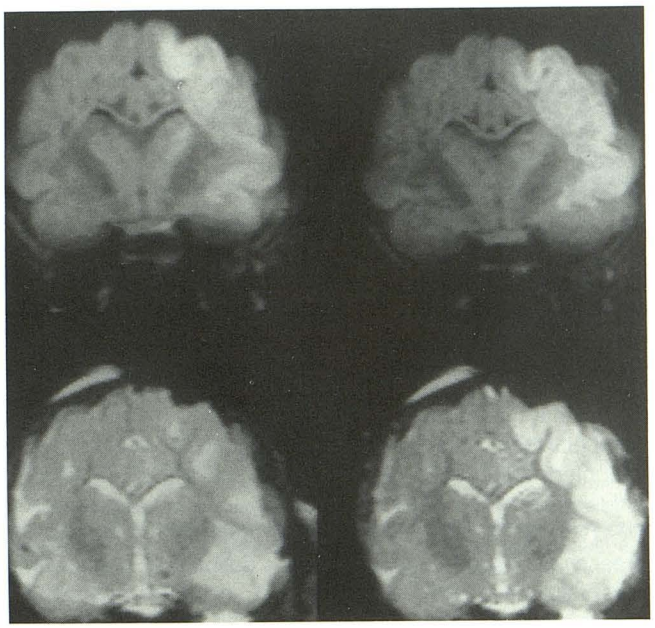

Fig. 2.—Diffusion-weighted coronal images 1800/80/4 (3-mm slice, 1-mm slice gap, FOV=80 mm, b = 1413 sec/mm^2) at level of optic chiasm 1 hr (*upper left*) and 5 hr (*upper right*) after MCA occlusion. Compared with contralateral control regions, signal intensity ratios increased by 55%, 60%, and 30%, measured in gray matter in the ectosylvian gyrus, middle temporal gyrus, and caudate nucleus, respectively, 1 hr after stroke. Corresponding T2-weighted spin-echo images 2800/160/2 (3-mm slices, 1-mm slice gap, FOV=80 mm) are shown in lower panels. 1 hr after stroke was induced, the T2-weighted image (*lower left*) shows only subtle mass effect in the temporal cortex ipsilateral to the occlusion. Measured relative signal intensity ratios increased by 16% in the gray matter of the ectosylvian gyrus, 24% in the middle temporal gyrus, and 10% in the caudate nucleus. At 5 hr after occlusion (*lower right*), hyperintensity is seen throughout MCA territory, although the signal intensity ratio of ischemic/nonischemic regions is substantially lower than the corresponding diffusion-weighted image (*upper right*).

5 hr after MCA occlusion (right panels), are shown for a single representative animal. The T2 tissue signal intensity ratio in the MCA territory ipsilateral to the occlusion was not significantly different from the contralateral normal hemisphere at 1 hr after stroke (lower left panel). By comparison, the signal intensity ratio in the corresponding diffusion-weighted image (upper left panel) was significantly elevated in the cortical and subcortical gray matter.

Five hours after MCA occlusion, T2-weighted images clearly demonstrated tissue injury, including increased mass-effect and hyperintensity (edema) throughout the MCA territory (Fig. 2, lower right panel). The anatomic distribution of increased signal intensity was similarly widespread on diffusion-weighted MR images (Fig. 2, upper right panel). Signal enhancement was observed in both parietal and temporal cortical areas inferior to the middle parietal gyrus, the medial aspect of the head of the caudate, and the lateral part of the globus pallidus. More posteriorly, there was extensive cortical and subcortical involvement of gray matter. A small region of hyperintensity was often seen in the inferior lateral sulcus, extending onto the temporal part of the occipital pole. A continuing close anatomic correspondence between diffusion-weighted and T2-weighted hyperintensity was seen 9 hr and 12 hr (Fig. 3) after occlusion. There was also close correspondence between the areas of high signal intensity on diffusion-weighted and T2-weighted MR images after MCA occlusion, and the distribution of ischemic tissue injury shown in subsequent TTC-stained coronal sections (Fig. 4).

The time course of changes in bioenergetic status induced by stroke was monitored by surface coil MR spectroscopy in all cats. Within 1 hr after occlusion, abnormal phosphorus-31 and proton metabolite ratios, determined from the Pii/PCr and lactate/NAA peak area ratios, respectively, were found (Fig. 5). Hyperintensity observed on diffusion-weighted MR images was closely associated with elevated lactate/NAA and Pii/PCr on MR spectroscopy, whereas no clear temporal relationship was found between the MR spectroscopy results and T2-weighted MR imaging at the early time points (up to about 2 hr).

Correlation of Regional Perfusion Deficits with Diffusion-Weighted MR Imaging

The purpose of the experiments with Dy-DTPA-BMA was twofold. First, we wanted to establish whether a nonionic T2*

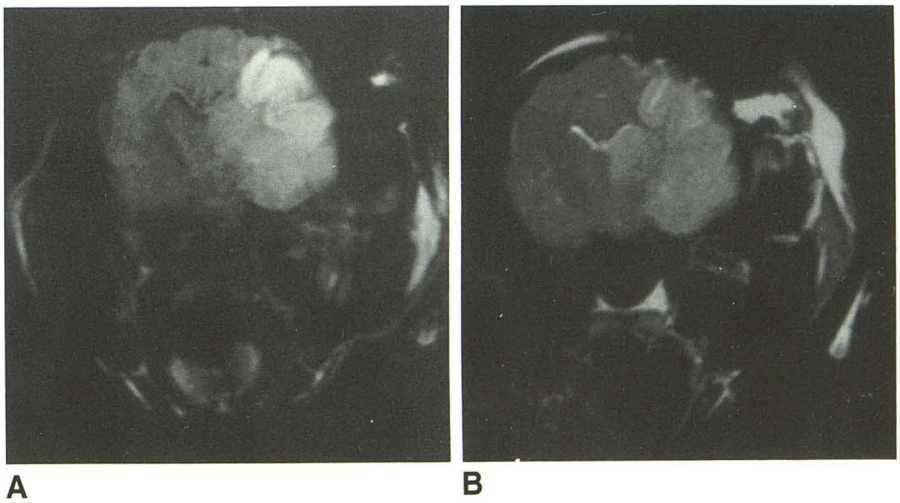

Fig. 3.—*A* and *B*, 12 hr after MCA occlusion, the diffusion-weighted (*A*) and T2-weighted (*B*) images show hyperintensity throughout ischemic MCA territory. Note, however, that the signal intensity ratio of the ischemic/nonischemic regions remains higher in the diffusion-weighted images. Same animal and MR parameters as Fig. 2.

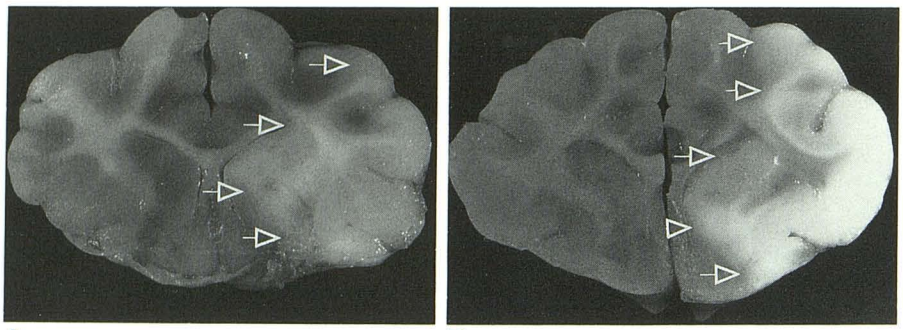

Fig. 4.—*A* and *B*, Triphenyl tetrazolium chloride (TTC)-stained coronal sections of cat brain show areas of ischemic damage at 5 hr (*A*) and 12 hr (*B*) after permanent unilateral occlusion of MCA. Ischemic or infarcted tissues (*arrows*), which lack viable electron transport chain enzymes, appear white. Note the close correspondence of the injured area with regions of hyperintensity in the diffusion-weighted and T2-weighted images (Fig. 3).

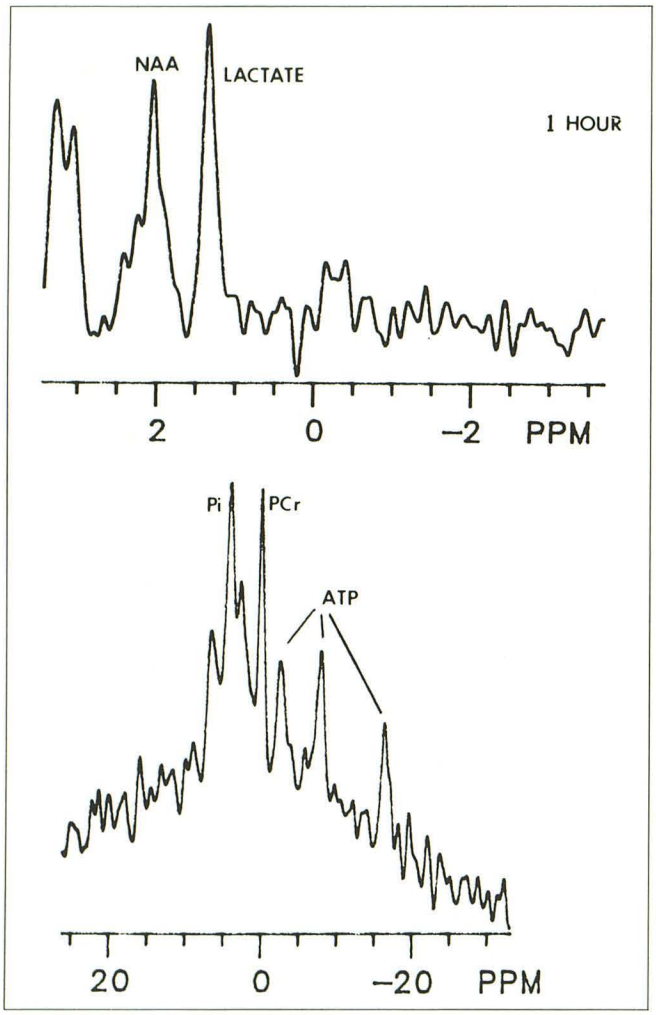

Fig. 5.—Proton (*top*) and phosphorus-31 (*bottom*) spectra obtained with a surface coil placed over the ischemic MCA territory 1 hr after unilateral arterial occlusion in same cat as Fig. 2. Evidence of metabolic injury is shown by the increased Pii/PCr and lactate/NAA ratios obtained from a surface coil placed on the skull over the ischemic parietal lobe. The abnormal phosphorus-31 and proton and metabolite ratios suggest that the hyperintensity observed on diffusion-weighted images 1 hr after occlusion is related to a disruption of normal oxidative phosphorylation in the MCA territory.

magnetic susceptibility contrast agent would allow early detection of ischemia-induced perfusion deficits using standard T2-weighted spin-echo MR imaging. Second, we wanted to compare anatomically the regions of perfusion deficits demonstrated with Dy-DTPA-BMA contrast-enhanced T2-weighted MR images with areas of high signal intensity on diffusion-weighted MR images. Using a 1 mmol/kg dosage of Dy-DTPA-BMA, we observed maximum signal intensity decreases of 35% in the gray matter of the normal, nonischemic cerebral hemisphere during the first 15 min after injection. No signal intensity changes were observed in the cortical and subcortical gray matter ipsilateral to the MCA occlusion, which consequently appeared bright on the postcontrast T2-weighted images. Signal intensity changes in the internal capsule of both the normal and ischemic hemispheres were relatively small, but the centrum semiovale was noticeably affected. At 45 min after administration of contrast material, signal intensity had recovered to over 90% of precontrast control values in all cerebral tissues (Fig. 6).

Perfusion deficits resulting from occlusion of the MCA were detected as a relative T2-weighted MR image hyperintensity of the ischemic tissues compared with the normally perfused areas in the contralateral hemisphere. Relative hyperintensity was found in the ischemic basal ganglia as early as 30 min after occlusion for both the 1 mmol/kg and 0.5 mmol/kg doses (Fig. 7). Signal differences between ischemic and contralateral control tissues were observed for gray matter and, to a lesser extent, for the white matter in the internal capsule. By comparison, T2-weighted MR images without contrast failed to demonstrate any significant signal differences prior to the detection of cerebral edema (signal hyperintensity) approximately 2–3 hr after MCA occlusion.

Regions of perfusion deficiency correlated well anatomically with areas of high signal intensity on diffusion-weighted MR images from the earliest (30 min) to the latest (12 hr) postocclusion observation periods employed in this study. An example of the close correspondence in anatomy between the region of perfusion deficit and diffusion MR image-determined area of tissue injury 5 hr after MCA occlusion is shown in Fig. 8.

Discussion

Early Detection of Ischemic Brain Injury

The results of this study confirm and extend our previous report [2] that diffusion-weighted MR imaging can significantly advance the time of detection of cerebral ischemic insults. In the present investigation evidence of stroke was seen in the

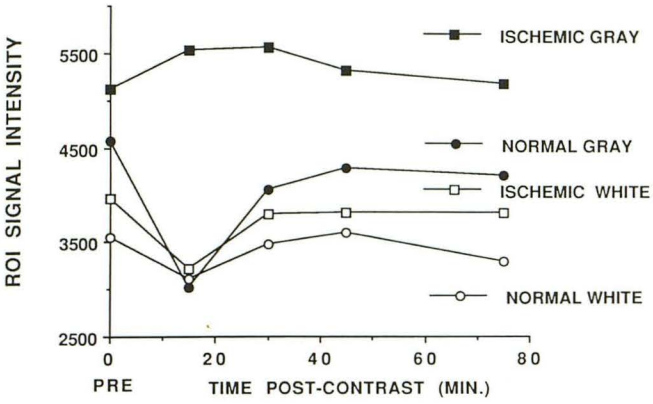

Fig. 6.—Signal intensity changes measured in normal and ischemic brain regions of one cat using a T2-weighted spin-echo pulse sequence 2800/160/2 after administration of 1 mmol/kg Dy-DTPA-BMA IV 1 hr after MCA occlusion. The susceptibility-induced signal attenuation was most prominent 15 min after contrast injection except in the nonperfused gray matter ipsilateral to the MCA occlusion. Signal attenuation washout occurred in all tissues within approximately 60 min after Dy-DTPA-BMA injection.

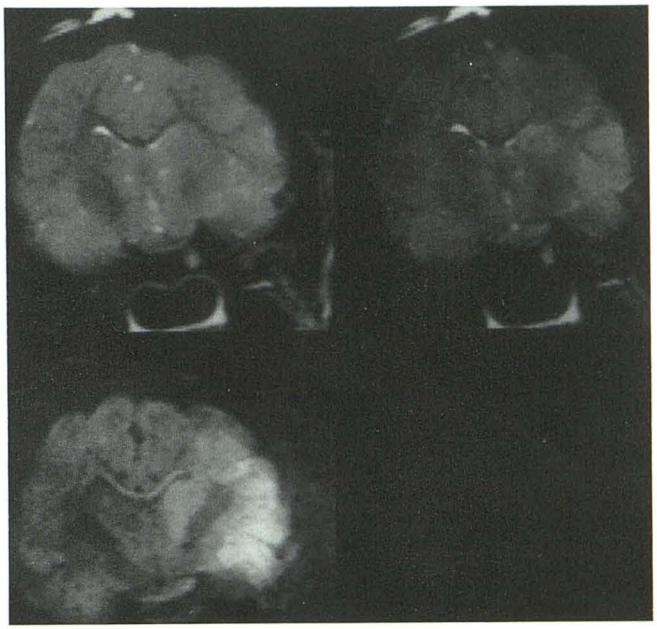

Fig. 7.—T2-weighted spin-echo images before (*upper left*) and after (*upper right*) administration of 0.5 mmol/kg Dy-DTPA-BMA approximately 1 hr after occlusion of right MCA. Corresponding diffusion-weighted image is shown at *lower left*. On the diffusion-weighted MR image, relative signal intensity ratios increased in the gray matter by 159% in the ectosylvian gyrus, 94% in the middle temporal gyrus, and 100% in the caudate nucleus. Corresponding signal intensity ratios increased in the magnetic susceptibility-enhanced MR image by 74%, 39%, and 101%, respectively. By comparison, the T2-weighted MR image without contrast did not clearly demonstrate the region of tissue injury at this early time.

MCA territory as early as 45 min following occlusion using diffusion-weighted MR images, whereas T2-weighted spin-echo images without contrast did not demonstrate increased signal intensity until 2–3 hr after occlusion. A close correlation was also found between diffusion-weighted tissue signal intensity increases and abnormal phosphorus-31 and proton metabolite ratios, which suggests that the hyperintensity seen after ischemia is likely related to a disruption of normal oxidative phosphorylation.

Correlation with Perfusion Deficits

The close spatial correlation between the regions of diffusion-weighted MR image hyperintensity and areas of high signal intensity on T2-weighted images following Dy-DTPA-BMA administration suggests that this contrast agent has significant utility in the early detection of cerebral ischemic insults. Relaxivity of paramagnetic chelates like Dy-DTPA-BMA is influenced by molecular diffusion through microscopic heterogeneous magnetic fields [6]. Chelates that have poor longitudinal relaxation but large magnetic moments produce contrast enhancement through loss of spin-echo signal intensity. Since Dy-DTPA-BMA remains in the intravascular compartment and its concentration within patent blood vessels is relatively uniform, signal intensity should be proportional to the fractional voxel volume occupied by vessels containing the agent. This magnetic susceptibility mechanism of MR contrast enhancement thus has the notable advantage of demarcating regions of deficient blood flow without crossing the blood-brain barrier. The results of the present study confirm our previous report [7] that intravenous Dy-DTPA-BMA can significantly advance the time of detection of cerebral ischemic insults caused by perfusion deficits.

Nature of Diffusion-Weighted MR Hyperintensity

The measured apparent diffusion coefficient in the hyperintense ischemic brain regions was approximately half that in the contralateral MCA territory, indicating slower microscopic proton diffusion [1, 2]. Motion artifacts, which can present severe problems for diffusion-weighted images [1, 8], were largely eliminated in the present investigation by a combination of barbiturate anesthesia, immobilization of the head in a restraint device, and the use of four or eight signal averages. The close temporal and anatomic correspondence between the appearance of hyperintensity on magnetic susceptibility-induced images and diffusion-weighted MR imaging suggests that the altered signal reflects stroke-induced perfusion deficits rather than motion artifact.

The precise origin of the hyperintense signal on diffusion-weighted MR images does, however, remain unclear. Several issues complicate the interpretation of the lower apparent diffusion coefficient in the occluded MCA territory. First, ischemic tissue injury is by its very nature multifactorial. It includes hypoxia, substrate deprivation, and toxic metabolite accumulation [9]. Second, cerebral tissues are composed of many different cell types that respond differently, and perhaps independently, to ischemia [10]. While no accurate data have been collected concerning the relative volumes occupied by neurons versus glia in cat cerebral cortex, one recent estimate is that they are about equal [11]. There is ultrastructural evidence that astrocytic glial swelling is an early event following cerebral ischemia [12, 13]. Increases in intracellular sodium, calcium, and chloride following stroke have generally been regarded as critical factors influencing astrocytic swelling [12, 14], but changes in extracellular K+ [15], lactic acid

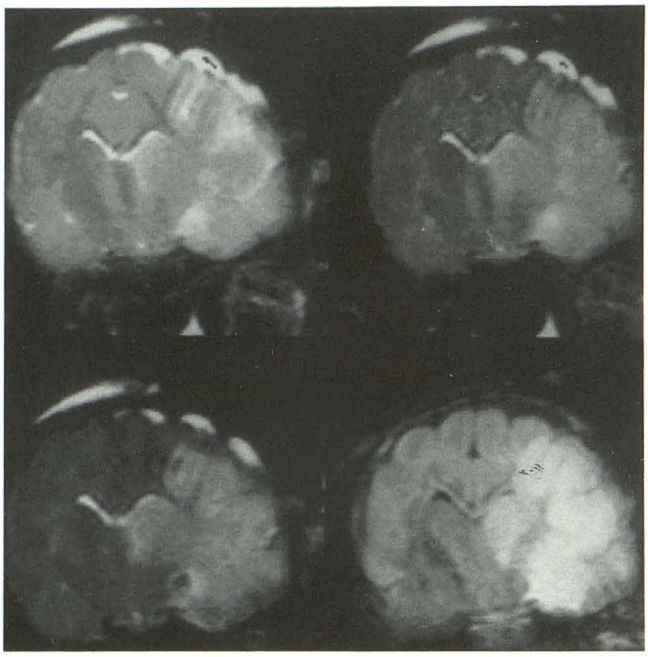

Fig. 8.—5–7 hr after MCA occlusion, hyperintensity was observed in the same anatomic regions on T2-weighted (*upper left*), diffusion-weighted (*lower right*), and magnetic susceptibility-enhanced (*upper right*) images15 min after injection of 0.5 mmol/kg Dy-DTPA-BMA and 15 min after 1.0 mmol/kg Dy-DTPA-BMA (*lower left* image). On precontrast T2-weighted MR image, signal intensity ratios increased by 109% in the ectosylvian gyrus, 18% in the middle temporal gyrus, and 39% in the caudate nucleus. The corresponding MR signal intensity ratios increased after injection of 0.5 mmol/kg Dy-DTPA-BMA by 83%, 34%, and 118%, respectively. After 1.0 mmol/kg Dy-DTPA-BMA, signal intensity ratios increased by 168%, 51%, and 211%, respectively. Finally, on the diffusion-weighted MR image, the corresponding increases in signal intensity ratios were 66%, 113%, and 61%, respectively.

and/or pH [16, 17], and free fatty acids and oxygen radicals [18] also play a role.

It is now known that severe focal ischemia causes both extra- and intracellular lactic acidosis, and that this acidosis is associated with gray matter edema predominantly affecting the astrocyte population of cells [16]. Astrocytes appear to be less resistant than neurons to acidosis and lose their normal morphology, membrane integrity, and cytoskeletal configuration with smaller drops in pH [19]. We have shown in preliminary experiments (Kucharczyk et al., unpublished results) that administration of calcium channel blockers preserved pre-ischemia concentrations of high-energy phosphates, maintained low levels of Pi and lactate, and also significantly reduced both tissue hyperintensity on diffusion-weighted images and histologically measured infarct size. This apparent drug-induced reversibility of diffusion-weighted image hyperintensity also indicates that the diffusion-weighted MR changes observed as early as 45 min after occlusion were not due to cell death. Considered together, these data suggest the possibility that ischemia may precipitate a loss of cellular volume control resulting from increased intracellular acidification of astrocytes as the primary event. Sodium ions taken up as a result of activated Na+/H+ transmembrane exchange would then cause water to flow into the intracellular compartment to maintain osmotic balance, resulting in cytotoxic edema, slower or restricted microscopic proton diffusion, and, consequently, hyperintensity on diffusion-weighted MR images.

Tissue osmolality changes following ischemia may also be a factor in the observed diffusion MR image hyperintensity. Recent studies suggest that the osmotic pressure gradient between blood and brain may have an important influence on the development of ischemic brain edema. Hatashita and Hoff [20] demonstrated that a hydrostatic pressure gradient across the capillary develops within minutes after the onset of ischemia and represents the driving force for early accumulation of edema. The osmolality in normal brain cortical tissue is about 8 mOsm/kg higher than that of plasma [20]. Other studies have shown that a significant increase in osmolality of ischemic brain tissue occurs within 2–6 min following ischemia [21, 22]. The increased brain osmolality correlates with water content, and could therefore account, at least in part, for the early accumulation of edema and reduced apparent diffusion coefficient after ischemic injury.

Since there is a direct relationship between temperature and the diffusion coefficients that quantify thermal Brownian motion, it is also possible that the high-intensity signal observed on diffusion-weighted MR imaging may be related to temperature changes in the ischemic MCA territory. Le Bihan et al. [23] used a phantom heated inside a clinical 0.5-T whole body imaging system to demonstrate that a 1°C change in temperature corresponds to a 2.4% change in diffusion coefficient. Busto et al. [24] have demonstrated that intraischemic brain temperature may fall by up to 7°C following bilateral carotid/vertebral occlusion in the rat. Pre- or postischemia induction of brain hypothermia may actually confer a substantial cerebroprotective effect [25].

Although cerebral blood flow was not directly measured in the present study, the Dy-DTPA-BMA contrast-enhanced MR images suggest considerable regional heterogeneity in blood flow disturbances throughout the ischemic MCA territory. In nearly all cases, signal hyperintensity was observed earlier in the region of the basal ganglia than neocortex on both magnetic susceptibility-enhanced and diffusion-weighted MR images. On this basis, it would appear that nonanastomosing end-arterial tissues, such as the caudate and putamen, might undergo more rapid and greater drops in temperature, following ischemia, since no collateral circulation is available [26]. In collaterally perfused areas such as neocortex, on the other hand, reductions in tissue temperature may be offset by continued blood flow in the partially ischemic watershed regions. A reduction in brain tissue temperature could therefore theoretically account for the observed hyperintensity on diffusion-weighted MR images. Further studies are required, however, to precisely assess the relative importance of postischemic hypothermia to the increases in signal intensity observed on diffusion-weighted MR images.

Finally, another possibility is that physiological motions within the cranium related to arterial blood flow pulsations might contribute to the differences in apparent proton diffusion in normally perfused versus ischemic regions. A reduction in cerebral blood flow after MCA occlusion might attenuate

pulsatile brain motions, thereby leading to a decrease in apparent proton diffusion and an observed diffusion-weighted hyperintensity in the ischemic tissues.

In summary, in vivo diffusion-weighted MR imaging accurately characterized early-onset brain tissue abnormalities caused by cerebral ischemia. Changes in signal intensity induced by acute stroke were observed much earlier on diffusion-weighted MR images than on T2-weighted spin-echo images. Hyperintensity seen on diffusion-weighted MR images was closely associated with evidence of metabolic disruption obtained by MR spectroscopy, whereas no clear temporal relationship was found between the MR spectroscopy results and T2-weighted MR imaging. Finally, the results of studies with a T2* shortening contrast agent, Dy-DTPA-BMA, suggest that the diffusion-weighted intensity is related to cerebral perfusion deficits.

REFERENCES

1. LeBihan D, Breton E, Hallemand D, et al. Separation of diffusion and perfusion in intravoxel incoherent motion MR imaging. *Radiology* **1988**; 168:497–505
2. Moseley M, Cohen Y, Mintorovitch J, et al. Early detection of regional cerebral ischemic injury in cats: evaluation of diffusion and T2-weighted MRI and spectroscopy. *Magn Reson Med* (in press)
3. Hossmann KA, Sakaki S, Zimmerman V. Cation activities in reversible ischemia of the cat brain. *Stroke* **1977**; 8:77–81
4. Siedler E. New mitro-monotetrazolium salts and their use in histochemistry. *Histochem J* **1980**;12:519–530
5. Bose B, Osterholm JL, Berry R. A reproducible experimental model of focal cerebral ischemia in the cat. *Brain Res* **1984**;311:385–391
6. Cacheris W, Rocklage SM, Quay S, et al. *Radiology* **1988**;169:383
7. Moseley ME, Kucharczyk J, Kurhanewicz J, et al. Comparison of MR imaging after administration of dysprosium-based magnetic-susceptibility contrast media with diffusion-weighted MR imaging in evaluation of regional cerebral ischemia. *Radiology* **1989**;173(P):383 (abstr)
8. Merboldt KD, Bruhn H, Frahn J, et al. MRI of "diffusion" in the human brain: new results using a modified CE-FAST sequence. *Magn Reson Med* **1989**;7:423–429
9. Ljunggren B, Schutz H, Siesjo BK. Changes in energy state and acid-base parameters of the rat brain during complete compression ischemia. *Brain Res* **1974**;73:277–289
10. Hossman K-A. The pathophysiology of ischemic brain swelling. In: Inaba Y, Klatzo I, Spatz M, eds. *Brain edemia*. Berlin: Springer-Verlag, **1985**: 367–384
11. Dietzel I, Heinemann U, Luz HD. Relations between slow extracellular potential changes, clial potassium buffering, and electrolyte and cellular volume changes during neuronal hyperactivity in cat brain. *Glia* **1989**;2: 25–44
12. Kimelberg HK, Ransom BR. Physiological and pathological aspects of astrocytic swelling. In: Federoff S, Vernadakis A, eds. *Astrocytes*. Orlando: Academic Press, **1986**:129–166
13. Chiang J, Kowada M, Ames A, et al. Cerebral ischemia III. Vascular changes. *Am J Pathol* **1968;**52:455–476
14. Rothman SM, Olney JW. Glutamate and the pathophysiology of hypoxic-ischemic brain damage. *Ann Neurol* **1986**;19:105–111
15. Moller M, Mollgard K, Lund-Anderson H, et al. Concordance between morphological and biochemical estimate of fluid spaces in rat brain slices. *Exp Brain Res* **1974;**22:299–314
16. Siesjo BK. Membrane events leading to glial swelling and brain edema. In: Inaba Y, Klatzo I, Spatz M, eds. *Brain edema*. Berlin: Springer-Verlag, **1985**:200–209
17. Norenberg MD, Mozes LW, Gregarios JB, et al. Effects of lactic acid on astrocytes in primary culture. *J Neuropathol Exp Neurol* **1987**;46:154–166
18. Chan PH, Fishman RA. Free fatty acids, oxygen free radicals, and membrane alterations in brain ischemia and injury. In: Plum F, Pulsinelli W, eds. *Cerebrovascular diseases*. New York: Raven Press, **1985**:161–168
19. Goldman SA, Pulsinelli WA, Clarke WY, et al. The effects of extracellular acidosis on neurons and glia in vitro. *J Cereb Blood Flow Metab* **1989**; 9:471–477
20. Hatashita S, Hoff JT. Biomechanics of brain edema in acute cerebral ischemia. *Stroke* **1988**;19:91–97
21. Schuier JF, Hossmann KA. Experimental brain infarction in cats. II. Ischemic brain edema. *Stroke* **1980**;11:593–597
22. Bandaranayake MN, Nemoto ME, Stezoski W. Rat brain osmolality during barbiturate anesthesia and global brain ischemia. *Stroke* **1978**;9:249–254
23. Le Bihan D, Delannoy J, Levin RL. Temperature mapping with MR imaging of molecular diffusion: application to hyperthermia. *Radiology* **1989**; 171:853–857
24. Busto R, Dietrich WD, Globus MT, et al. Small differences in intraischemic brain temperature critically determine the extent of ischemic neuronal injury. *Cereb Blood Flow Metab* **1987**;7:729–738
25. Busto R, Dietrich WD, Globus MT, et al. The importance of brain temperature in cerebral ischemic injury. *Stroke* **1989**;20:1113–1114
26. Grand W. Microsurgical anatomy of the proximal middle cerebral artery and the internal artery bifurcation. *Neurosurgery* **1980**;7:151–159